UCRL-JC-131221
PREPRINT

Laser Damage Performance of Fused Silica Optical Components Measured on the Beamlet Laser at 351 nm

M. R. Kozlowski
R. Mouser
S. Maricle
P. Wegner
T. Weiland

This paper was prepared for submittal to the
30th Boulder Damage Symposium: Annual Symposium on
Optical Materials for High Power Lasers
Boulder, Colorado
September 28 - October 1, 1998

December 22, 1998

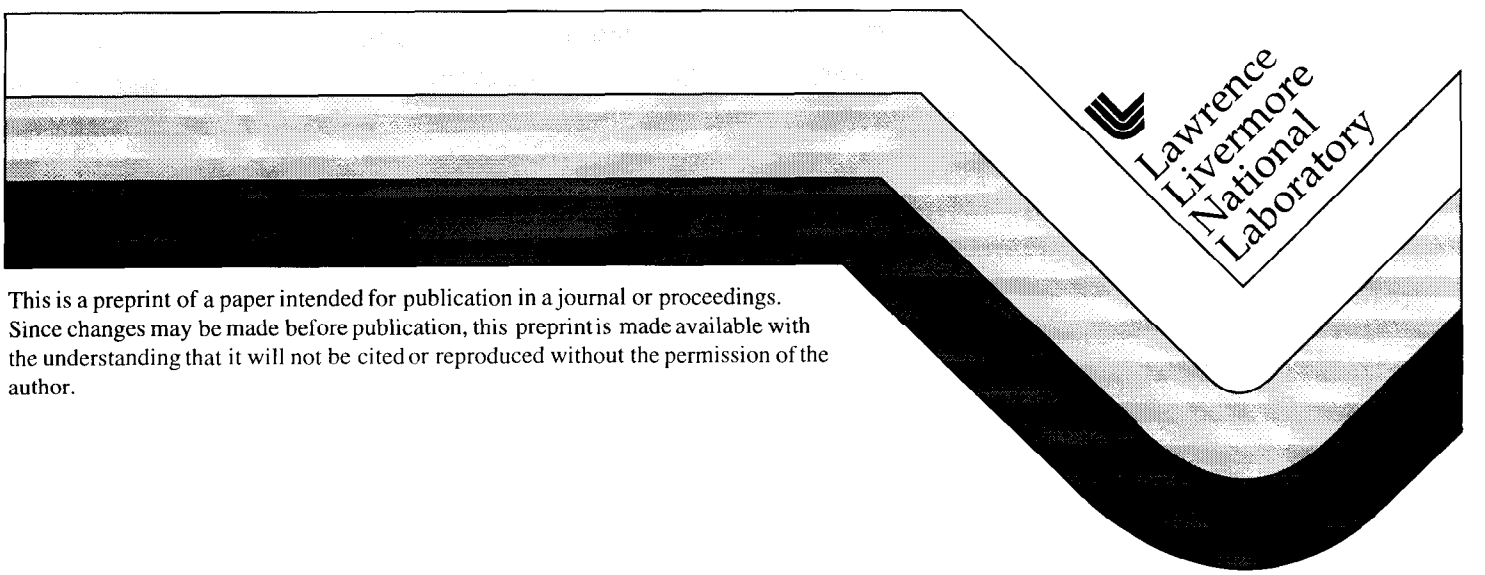

Laser Damage performance of fused silica optical components measured on the Beamlet Laser at 351 nm

M.R. Kozlowski, , R. Mouser, S. Maricle, P. Wegner and T. Weiland
Lawrence Livermore National Laboratory
7000 East Avenue, Livermore, CA 94551

ABSTRACT

A statistics-based model is being developed to predict the laser-damage-limited lifetime of UV optical components on the NIF laser. In order to provide data for the model, laser damage experiments were performed on the Beamlet laser system at LLNL (aperture: 34 cm x 34 cm). Three prototype NIF focus lenses were exposed to 351 nm pulses (1.5ns or 3ns) during four experimental campaigns, each consisting of 23 to 38 pulses at NIF relevant fluences. Each lens was sol-gel AR coated and all laser exposures were performed in a vacuum environment. Through inspections of the lens before, during and after the campaigns, pulse-to-pulse damage growth rates were measured for damage initiating both on the surfaces and at bulk inclusions. Radial growth rates measured for rear surface damage was typically 10x higher than that measured in the bulk or at the front surface. No significant correlation of growth rate to precursor type was indicated. For 5 J/cm^2, 3 ns pulses the typical radial growth rate was nominally 20 μm/pulse. Average growth rates measured on three lenses made by two manufacturers were in good agreement. While the growth rate clearly increased with fluence, the data obtained was insufficient to quantify the dependence. The growth rates reported here were 20x -50x higher than values predicted from off-line studies of bare surfaces in air.

Key words: laser damage, fused silica, polishing, NIF, growth rate, defects, inclusions

1. INTRODUCTION

Under the aggressive illumination conditions of the National Ignition Facility (NIF) laser some laser-induced damage is expected to occur in the fused silica optics transmitting UV laser light (351 nm or 3ω) to the target. These UV optics include the focus lens, diffractive optics plates (DOPs) and the debris shield. Combined with the KDP crystals used for frequency conversion, these optics make up the NIF final optics assembly (FOA). In order to evaluate the performance of final optics components, a testbed system, called the Mule, was added to the Beamlet laser system at LLNL.[1]

The goal of the experiments described here was to study the evolution of UV laser damage on final focus lenses within the Beamlet Mule during four 3ω campaigns. Information gained includes the density of damage sites on the optics and the rate of growth of the damage sites when exposed to additional laser pulses. This paper addresses the damage growth issue, examining such parameters as fluence, damage location (input, bulk, or output surface) and precursor type. Another paper in these proceedings by Feit et al.[2] discusses the concentration of damage sites on the lens and our ability to predict that damage concentration based on off-line testing using 1mm diameter beams. Both types of information are being used to develop a model for optics functional lifetime on the NIF laser.

Studies by Salleo, et al.[3], primarily at 1ω, have indicated that the radius, r , of a laser damage site on fused silica grows as

$$r = N \cdot R(F) \qquad (1)$$

where N is the number of pulses and R is the growth rate in μm/pulse. R is a linear function of the fluence, F, in J/cm^2. A constant radial growth rate varying linearly with fluence is consistent with a simple geometric model based on uniform absorption in a thin absorbing layer on the surface of a hemispherical damage pit. The absorbing layer could be SiO or Si produced by the decomposition of SiO_2 at high temperatures. The hemispherical pit model is somewhat of a simplification, however, because damage sites observed on large 3ω optics typically have aspect ratios of 3.1:1 rather than 2:1 as expected for a hemispherical pit.[4] Real damage sites also tend to be somewhat irregular in shape, often with cracks radiating from the main damage site. The growth rate R may also depend on parameters such as the nature of the damage initiator and the environment of the optic (air or vacuum). In the present experiment R(μm/pulse) was determined for AR-coated NIF-scale fused-silica focus lenses illuminated in a vacuum environment (the final optics environment in NIF).

2. DAMAGE TESTING AND OPTICS INSPECTION

2.1 Fused silica lens heritage and off-line characterization.

Three different lenses were used in the series of tests. All lenses used had plano input surfaces and aspheric output surfaces. The lenses are 39cm x 39cm x 2.5cm (center). Table 1 provides a summary of the four 3ω campaigns and the lens used in each. The lens identifier includes the serial number and a letter identifying the vendor that made the lens. Vendors A and B used different polishing compounds and different polishing and post-polishing processes. For vendor A, off-line testing also showed that there was significant improvement in the damage performance of lens 04A relative to 02A as a result of polishing process improvements. It will be shown below that in spite of these difference all lenses showed similar growth rates at fluence of 5-6 J/cm^2.

Table 1: Beamlet 3ω campaign shot history and average damage growth data. Also noted is the number of sites used to calculate the growth rates for each campaign.

Campaign	1 (MDT)	2 (HDT1)		3 (Tripling)	4 (HDT2)			Number of sites used in growth rate calculations			
sub-campaign		a	b		a	b	c+d				
Lens	02A	04A		01B	01B						
# of pulses	26	13	10	38	10	6	7				
pulselength	3 ns	3 ns	3 ns	1.5 ns	3 ns	3 ns	3 ns				
Avg. Fluence, J/cm^2	5.1	5.1	5.6	2.5	5.1	7.1	7.0				
location	Average radial growth rate, μm/pulse							1	2	3	4
rear	18.3	19.3	49.4	4.4	26.0	120.2	135.8	9	13	11	17
bulk	4.2			0.8	1.9	5.9	3.0	4		2	2
front	2.6			0.7	1.1	5.0	4.9	5		5	4
							Total:	18	13	18	23

Prior to installation on the Beamlet laser each lens was cleaned, mapped using a Defect Mapping System (DMS) and coated with a sol-gel AR coating. The lenses were again DMS mapped after being removed from Beamlet following each campaign. The DMS uses fiber optic light bars to internally illuminate the optic through the four edges.[5] A full aperture image of the optic is taken using a mega-pixel CCD camera. The system allowed detection of defects as small as 10μm over the full 40cm x 40cm optic. Due to blooming of the defects in the image, it is not possible to resolve the size or features or the individual defect/damage sites directly from the mega-pixel map. After identification of defects in the image, a long focal length microscope is used to photograph individual sites. The resolution of the micrographs is ~5 μm. Damage sites are characterized by their location on the optic and any precursor that the damage site could be associated with. Front and rear damage corresponds to the laser input and output surfaces of the lens, respectively.

2.2 Beamlet Campaigns and in-situ characterization

The average fluences, pulselengths and numbers of pulses involved in the Beamlet campaigns are summarized in Table 1. All campaigns except Campaign 3 used 3ns square pulses. For all campaigns the typical peak-to-average beam modulation was 1.3-to-1. For Campaigns 1 to 3 the beam aperture was 34 cm x 34 cm. For Campaign 4 the beam size was 30 cm x 30 cm.

At two times during each Campaigns 2 and 4 the Mule was vented so that in-situ inspections of the lens could be performed. The fluences and number of shots comprising the sub-campaigns between inspections are listed in Table 1. In-situ inspections used a CCD camera and microscope to record images of laser-induced damage sites. Initially two cameras were used to record images at ~3mm and ~9mm FOV without repositioning the microscope. By the end of the campaigns only a ~6mm FOV system was used. An Infinity K2 long working distance (30 cm) single-camera microscope was used in these efforts. The microscope assembly was bagged for cleanliness and mounted on a X-Y rail system for coordinate measurements. All images were taken from the output side of the lens. The lens was also lit from the output side using an

intense fiber light held close to the damage, diffusely scattering light into the camera. The damage location (X-Y coordinate plus front, rear or bulk), diameter and morphology were recorded for each site measured.

Figure 1 shows an example of a DMS image of lens 01B following Beamlet Campaign 3. The 33 sites that were studied during the various inspections in Campaigns 3 and 4 are indicated. Most of the sites in the lower left corner were initiated in off-line damage testing prior to the Beamlet Campaigns.

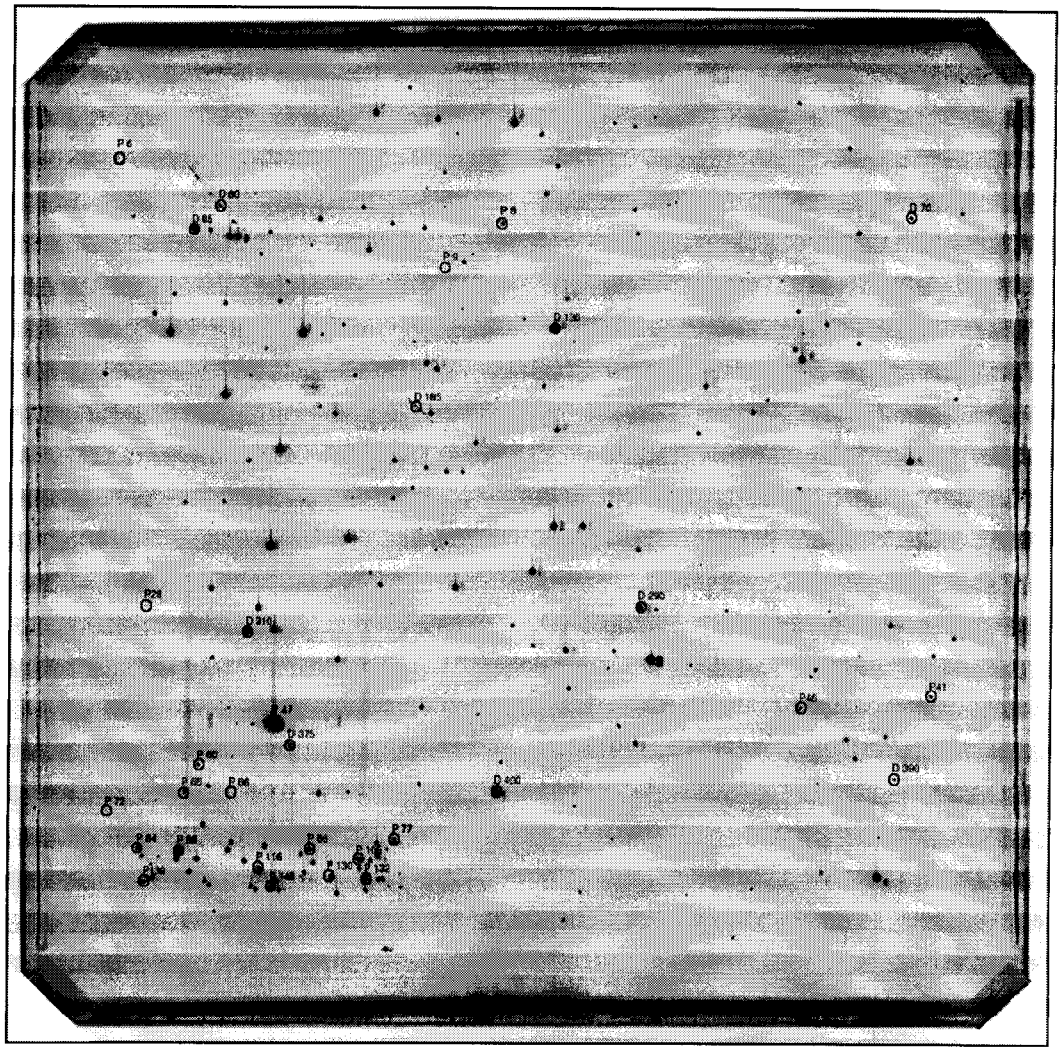

Figure 1. DMS map of lens 01B following Beamlet 3ω Campaign 3 (Tripling) . The map shows the location of the 33 damage sites studied during Campaigns 3 and 4. As a result of camera blooming the damage sites appear larger than they actually are.

The damage growth rates were categorized by the type of precursor that initiated the damage, if known. The precursors types included: surface scratches and digs (pin-point defects), bulk inclusions, and damage sites from off-line testing (with unknown precursors). It should be noted that for high-quality prototype NIF optics most damage sites cannot be correlated to a known precursor.

Micrographs showing the evolution of a single damage site on lens 01B during Campaigns 3 and 4 are shown in figure 2. The damage size is measured at the largest width of the damage site. Note that the damage sites have an irregular and changing shape so there is some inherent variability in the measurements. For many of the sites studied additional damage

features appear within the field of view of the micrographs. It is possible that these sites are initiated by contamination from debris from the primary site. Examinations of larger fields of view, however, do not indicate secondary distributions of damage sites surrounding primary larger sites. The additional damage sites may instead be due to the expected initiation of new damage sites each time the fluence is increased.

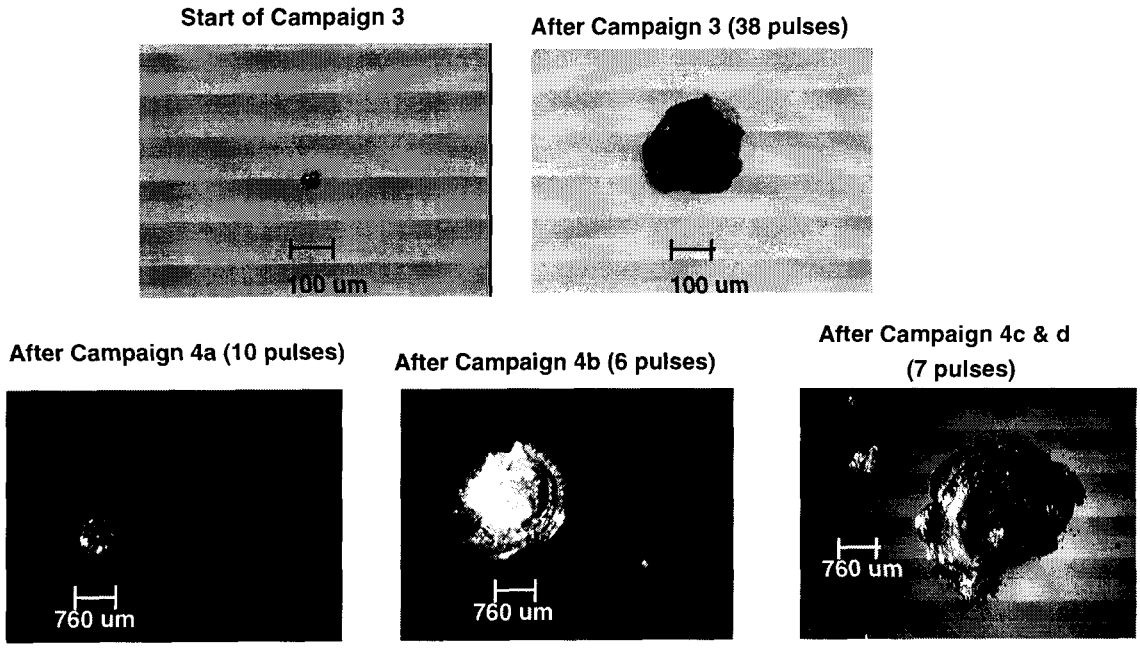

Figure 2: Optical micrographs showing the evolution of a single damage site studied during Campaigns 3 and 4.

Several of the rear surface damage sites studied here are correlated with damage at inclusions in the bulk of the fused silica. High-index bulk inclusions in fused silica are known to cause beam focusing and consequent bulk damage at or near the rear of the inclusion.[6] The bulk damage site then further modulates the beam resulting in damage to the optics rear surface. The inclusion-induced damage process is shown schematically in figure 3. Micrographs of a bulk damage site and the resulting bulk and rear damage sites are shown in figure 4.

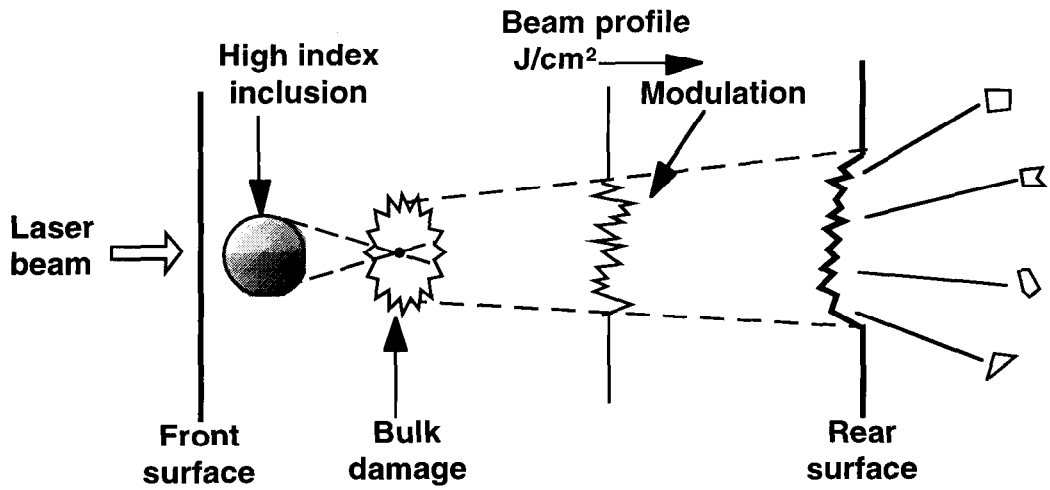

Figure 3: Schematic model of inclusion-induced bulk and rear-surface damage in fused silica.

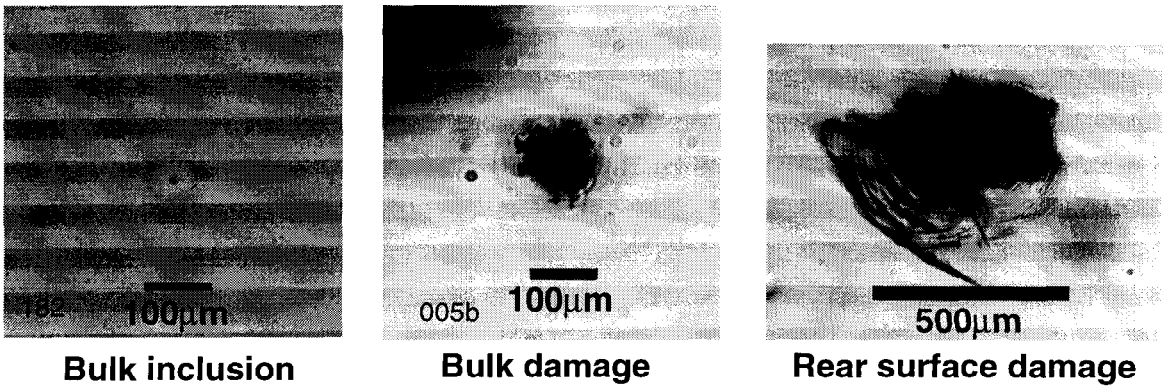

Figure 4: Micrographs of a bulk inclusion in fused silica and the bulk and rear-surface damage morphologies resulting from 3ω illumination.

Radial damage growth rates (μm/pulse) in fused silica have been shown to increase linearly with fluence.[3] An average growth rate over a series of pulses can therefore be associated with the average fluence within that series. Growth rates presented here are simply calculated as the change in damage size between inspections divided by the number of pulses.

3. DAMAGE GROWTH RESULTS

3.1 Results from Beamlet Campaigns

Damage results from Campaign 1 have been reported in detail in ref. 7. That study concluded that rear-surface damage sites, particularly those initiated at scratches, had the highest growth rates. The average growth rates measured in Campaign 1 are summarized in Table 1 along with the results from the other campaigns. The following discussion will focus on Campaigns 3 and 4 where the majority of the data was obtained.

Figure 5 compares the growth rates measured for the 16 damage sites studied in both Campaigns 3 and 4a. The growth rates for Campaign 3, which had an average fluence of 2.5 J/cm^2 were ~10x lower than those of Campaign 4a which had an average fluence of 5.1 J/cm^2. The data points form a rough line indicating that the relative growth rates of damage sites are constant from campaign to campaign. The plot shows that rear surface growth rates are consistently higher than front surface growth rates. This later observation is consistent with results reported by Salleo et al.[3] and the results from Campaign 1.

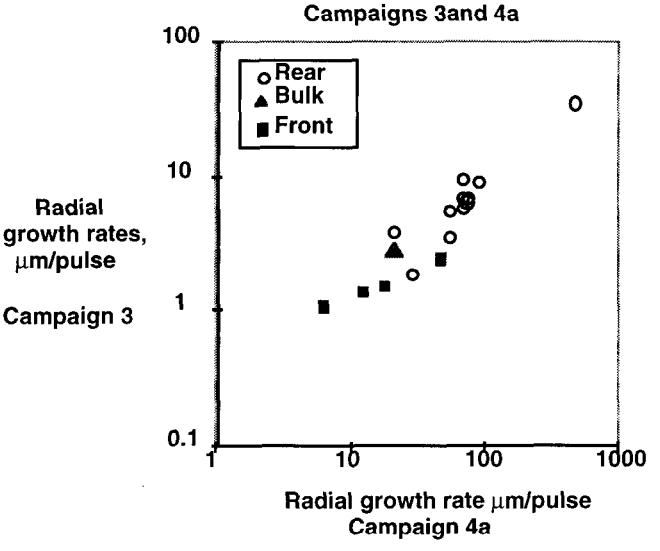

Figure 5: Growth rates measured for the 16 damage sites studied in both Campaigns 3 and 4a.

For rear-surface damage the range of growth rates indicated in figure 5 is greater than 10x. Assuming that the growth rate varies linearly with fluence, a variation of 2x can be attributed to the 1.3-to-1 modulation of the beam. The remaining spread in the data is assumed to be due to differences in growth rates of individual sites. Figures 6 a and b show the range and average rear-surface growth rates measured for different categories of precursors. Both figures show increased growth rates for higher fluences. Figure 6a shows rear surface growth rates measured in Campaign 1 for three types of precursors: digs, scratches, and bulk inclusions. Figure 6b shows data from 17 rear-surface damage sites measured during Campaign 4. For both sets of data rear-surface growth rates associated with bulk inclusions provide the lowest growth rates. The variation, however, is small compared to the spread in the data. These attempts to correlate growth rates with known precursor types did little to clarify the range in observed growth rates. Because there was no correlation of known damage precursor types with rear-surface growth rates it is justifiable to combine data from all precursor types in summarizing data for individual surfaces.

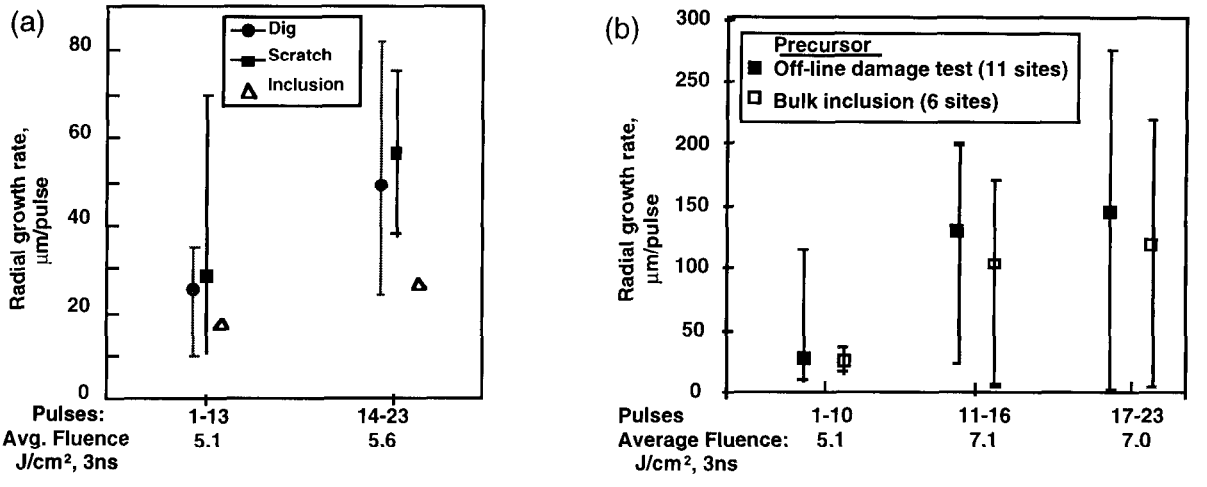

Figure 6: The range and average growth rates measured on rear surfaces for different types of precursors in (a) Campaign 1 and (b) Campaign 4

Average growth rates measured for front, rear and bulk damage sites during the four Beamlet UV campaigns are summarized in Table 1 and figure 7. The rear surface growth rates are ~10x higher than either the front surface for bulk damage growth rates. While there is a general increase in growth rate with fluence, a simple linear dependence is not obvious. It should be noted that there are two caveats to this data: 1) the data from Campaign 3 is for 1.5ns. While we assume that there is no pulselength dependence of growth rates (consistent with observations at 1.06 µm [3]) this has not been directly proven for 351 nm; 2) the data taken at fluences above 5.5 J/cm^2 is Campaigns 2 and 4 were obtained while anomalous damage was occurring on the KDP frequency conversion crystal. It is not known whether the KDP damage and associated debris influenced the growth rates on the upstream fused silica lens. While debris from the KDP damage has been correlated with some damage initiation on the lens, its impact on lens damage growth rates, particularly for the rear surface, is not obvious.

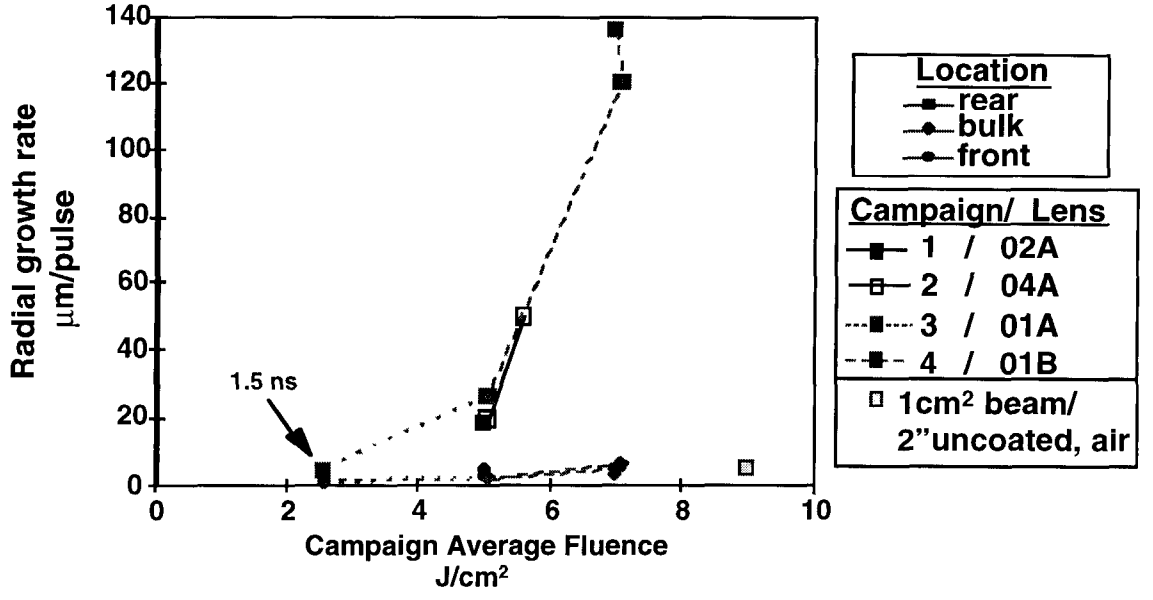

Figure 7: Plot showing the average surface and bulk growth rates measured during the four Beamlet 3ω campaigns. Also included is a single data point from an off-line test on an uncoated fused silica sample tested in air.

The growth rates measured near 5 J/cm^2 show good agreement among three campaigns using three different lenses made by two different manufacturers. The agreement suggests that the growth rate of damage in fused silica is a characteristic property of the bulk material, controlled by fused silica optical and thermomechanical properties rather than by the surface finish. In contrast the density of damage sites is strongly dependent on surface finish. It is also possible, however, that while the relative growth rates in the experiment were controlled by the material, the absolute growth rate was controlled by "system" properties of the Beamlet Mule such as potential surface contamination or the vacuum environment.

3.2. Comparison with off-line growth rate data

Several experiments have been performed to study damage growth rates using small (~1mm diameter) beams.[3] Most of these experiments were performed with 1.06μm illumination and focused on drilling rates rather than the lateral growth rates. These small-beam experiments provided useful information on the dependence of growth rates on fluence, pulselength and pulse repetition rate. However, the tests provide limited data for quantitative comparison with the large-beam 351nm growth rate data reported here.

The most relevant off-line 351 nm growth data for fused silica optics was obtained using the 1cm^2 beam of the LLNL Optical Sciences Laser (OSL).[8] A representative rear surface growth rate measured for 9 J/cm^2, 3ns pulses is included in figure 7. The OSL growth rate is 20 to 50 times lower than what might be expected from extrapolation of the Beamlet data to comparable fluences. Several differences between the Beamlet and OSL experiments must be noted. The Beamlet tests were done in a vacuum environment using a large-aperture sol-gel coated lenses produced by NIF-qualified vendors. The OSL study was performed in air on a 2" uncoated substrate prepared by another vendor. The influences of environment, AR coating and substrate source are not known. A series of experiments using a nominal 1cm^2 laser beam are being planned to address these issues.

4. CONCLUSION AND DISCUSSION

Laser damage growth rates were measured on three prototype NIF lenses illuminated at 351 nm, 1.5 ns or 3 ns pulses. Radial damage growth rates increased with fluence and were approximately 10x higher for rear surface damage sites than for those in the bulk or on the front surface. The significant spread in the growth rates measured for a particular location could not be attributed to a dependence on known precursor types. The similarity in average growth rates measured for the three lenses may suggest that the growth rate is a characteristic property of the fused silica and not of the surface finish. The spread in the data for a given location may be associated with the variation in the morphologies of the individual damage sites rather than on the precursors that originally caused the damage initiation. For high quality laser optics the absorbing

defect initiating the damage is likely less than 1 micron in size. It is unlikely that damage features with diameters of hundreds of microns have any memory of the initial damage initiators.

The factor of 20x to 50x difference between growth rates measured in an off- line test and those estimated from the Beamlet tests suggests an influence of extrinsic parameters such as the optic environment (air vs. vacuum) or the presence of an AR coating. Laser-induced damage to optical surfaces is generally associated with the creation of a plasma at the damage site. The interaction of the plasma with both the laser beam and the optic surface would be influenced by the environment of the optic. The presence of an optical coating could also influence that interaction, particularly in the case of sol-gel AR coatings which often show signs of contamination in vacuum environments.

When combined with information on the density of damage sites on an optic, the information on damage growth rate presented here can be used to develop a model for functional lifetimes of laser optics. Additional experiments and a supporting modeling effort are underway to clarify the dependence of damage growth performance on parameters such as use environment, surface coatings and laser characteristics (pulselength and shape, laser wavelength).

5. ACKNOWLEDGMENTS

The authors thank the ICF Optics Processing Group and Sheldon Schwartz for there efforts in preparing the optics discussed here and the Beamlet Operations crew for carrying out the Beamlet Campaigns.

Work performed under the auspices of the U.S. Department of Energy by Lawrence Livermore National Laboratory under Contract W-7405-ENG-48.

6. REFERENCES

1. S.C. Burkhart, K.R. Brading, P.M. Feru, M.R. Kozlowski, J.E. Murray, J.E. Rotherberg, B.M. Van Wonterghem, P.J. Wegner, T.L. Weiland, "High-fluence and High-Power 1.05 μm and 351 nm Performance Experiments on Beamlet," *Third Annual International Conference on Solid State Lasers for Application to Inertial Confinement Fusion*, SPIE vol. 3492, 1999.
2. M.D. Feit, A.M. Rubenchik, M.R. Kozlowski, F.Y. Genin, S. Schwartz, L. Sheehan, "Extrapolation of damage test data to preedict performance of large-area NIF optics at 355 nm," *these proceedings*, SPIE vol. 3578. See also M.D. Feit, et al. "Statistical evaluation of damage risks in NIF and LMJ optics at 355 nm," *Third Annual International Conference on Solid State Lasers for Application to Inertial Confinement Fusion*, SPIE vol. 3492, 1999.
3. F., Salleo, R. Chinsio, F. Y. Genin, "Crack propigation in fused silica during UV and IR ns-laser illumination," *these proceedings*, SPIE vol. 3578.
4. P. Ehrmann, "Damage diameter-to-depth (aspect) ratio in used Nova debris shields," LLNL internal communication, June 11, 1998. For 1ω Nova lenses the damage aspect ratio was 3.15-to-1.
5. F. Rainer, R.T. Jennings, J.F. Kimmons, S.M. Maricle, R.P. Mouser, S. Schwartz, C.L. Weinzapfel, "Development of practical damage-mapping and inspection systems," *Third Annual International Conference on Solid State Lasers for Application to Inertial Confinement Fusion*, SPIE vol. 3492, 1999.
6. Feit, M.D., Rubenchik, A.M., "Laser intensity modulation by nonabsorbing defects," *Laser-induced Damage in Optical Materials, 1996 - SPIE*, **2966**, 475-480, 1997.
7. M.R. Kozlowski, S. Maricle, R. Mouser, S. Schwartz, P. Wegner, T. Weiland "3ω damage threshold evaluation of final optics components using Beamlet Mule and off-line testing," *Third Annual International Conference on Solid State Lasers for Application to Inertial Confinement Fusion*, SPIE vol. 3492, 1999.
8. D. Milam and F. Genin, unpublished results, LLNL, September 1997.